

DETC2013-12600

## WAVE ENERGY EXTRACTION MAXIMIZATION IN IRREGULAR OCEAN WAVES USING PSEUDOSPECTRAL METHODS

Daniel R. Herber, James T. Allison

University of Illinois at Urbana-Champaign  
 Industrial and Enterprise Systems Engineering, Urbana, IL 61801  
 Email: {herber1, jtalliso}@illinois.edu

### ABSTRACT

Energy extraction from ocean waves and conversion to electrical energy is a promising form of renewable energy, yet achieving economic viability of wave energy converters (WECs) has proven challenging. In this article, the design of a heaving cylinder WEC will be explored. The optimal plant (i.e. draft and radius) design space with respect to the design's optimal control (i.e. power take-off trajectory) for maximum energy production is characterized. Irregular waves based on the Bretschneider wave spectrum are considered. The optimization problem was solved using a pseudospectral method, a direct optimal control approach that can incorporate practical design constraints, such as power flow, actuation force, and slamming. The results provide early-stage guidelines for WEC design. Results show the resonance frequency required for optimal energy production with a regular wave is quite different than the resonance frequency found for irregular waves; specifically, it is much higher.

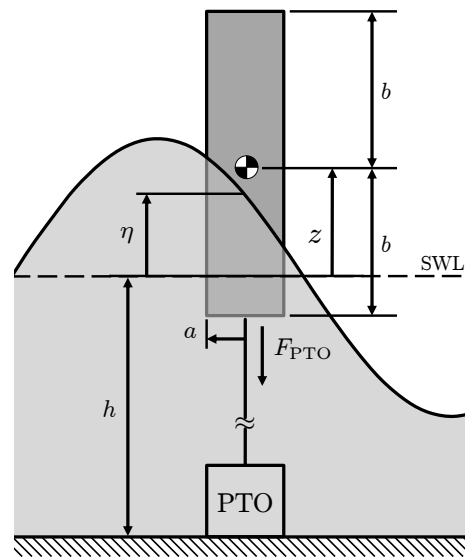


FIGURE 1: Heaving cylinder wave energy converter.

### 1 Introduction

Ocean waves have the highest energy density among renewable resources. Energy extraction from ocean waves relies on dynamics, i.e. the destructive interference between the waves and the oscillation of the wave energy converter (WEC) [1]. Diverse WEC designs have been investigated, particularly over the course of the last four decades (see Ref. [2] for early work). Reviews of available WEC tech-

nologies are available in Refs. [1, 3, 4].

In this article we focus on the heaving cylinder WEC (HCWEC) connected to a power take-off (PTO) moored to the ocean floor (Fig. 1), similar to the systems described in Refs. [5, 6]. The cylinder radius is  $a$ , while the draft of the cylinder,  $b$ , is the submerged length in still water. In order to simplify the design, the buoy is assumed to be of

constant density and of length  $2b$ . Therefore, the vertical position of the buoy mass center  $z$  is measured from the still water level (SWL), which is  $h$  meters above the ocean floor. The wave elevation is denoted  $\eta(t)$ . As buoyancy forces the heaving cylinder upward, motion is resisted by the PTO. Work is done on the PTO at the rate

$$P(t) = F_{\text{PTO}}(t)\dot{z}(t), \quad (1)$$

where  $F_{\text{PTO}}(t)$  is the PTO force and  $\dot{z}(t)$  is the vertical velocity of the heaving cylinder. This system is similar to a point absorber, i.e., heaving body WECs that are much smaller than ocean wavelength  $\lambda$  and have only one mode of oscillation in the vertical direction [2, 7]. Here the HCWEC design objective is defined as maximizing the energy absorbed over a desired time horizon  $t_0 \leq t \leq t_f$ :

$$\max \int_{t_0}^{t_f} P(t)dt, \quad (2)$$

where the time horizon is defined between  $t_0$  and  $t_f$ . Many studies treat  $\eta$  as a regular wave (e.g.  $\eta(t) = A\sin\omega t$ ) [8]. However, real ocean waves are not regular but irregular. The key to producing a successful WEC is maximizing energy capture in irregular ocean waves.

### 1.1 Irregular Ocean Waves

An irregular incident wave field can be modeled with a linear superposition of a finite number of linear Airy wave components [9]. The surface elevation relative to the SWL at a fixed position is approximated by

$$\eta(t) = \sum_{i=1}^{N_I} \eta_i(t) = \sum_{i=1}^{N_I} \frac{H_i}{2} \sin(\omega_i t + \theta_i), \quad (3)$$

where  $N_I$  is the number of regular wave components used to represent the irregular wave field, and  $H_i$ ,  $\omega_i$ , and  $\theta_i$  are the wave height, angular frequency, and phase for component  $i$ , respectively. The wave phase components,  $\theta_i$ , are random phase shifts. Increasing  $N_I$  will improve the fidelity of the wave field approximation. McTaggart noted that a minimum of 20 wave components is needed to ensure accurate modeling of an irregular seaway [10].

A wave spectrum, denoted  $S(\omega)$ , is required to define the heights and frequencies of the wave components used to construct  $\eta$  in Eqn. (3). The amplitude of the  $i$ th component is:

$$A_i = \frac{H_i}{2} = \sqrt{2S(\omega_i)\Delta\omega_i}, \quad (4)$$

where  $\Delta\omega_i$  is the wave frequency interval for component  $i$ . The wave spectrum can be found experimentally for a particular location or empirical expressions can be used [11]. One common standardized spectrum is the Bretschneider (BS) spectrum that describes a developing sea. It is also known as the two-parameter ITTC spectrum [12]. The spec-

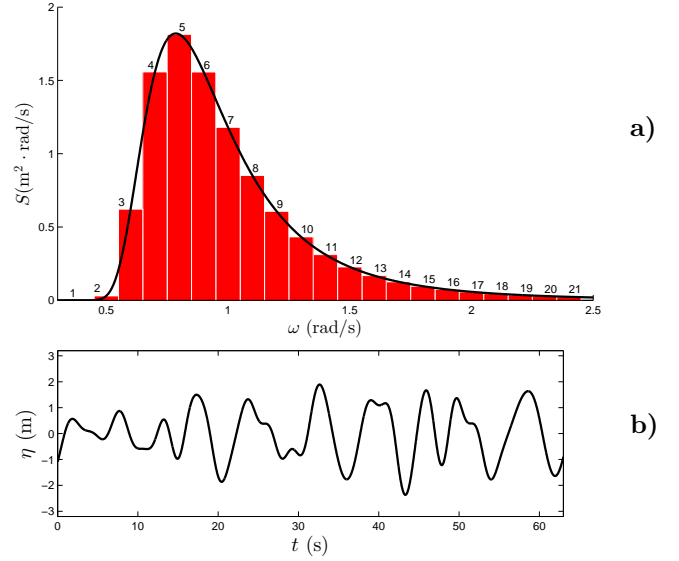


**FIGURE 2:** Bretschneider spectrum with  $H_{1/3} = 4$  m and  $T_p = 8$  s where **a)**  $S(\omega)$  and **b)**  $\eta(t)$ .

trum has the general form:

$$S(\omega) = \frac{\alpha}{\omega^5} e^{-\beta/\omega^4}, \quad (5)$$

where  $\alpha$  and  $\beta$  are the empirical coefficients given by:

$$\alpha = 487 \left( \frac{H_{1/3}}{T_p^2} \right)^2, \quad \beta = \frac{1948.2}{T_p^4}, \quad (6)$$

where  $H_{1/3}$  is the mean wave height of the highest third of the waves, and  $T_p$  modal period or the period associated with peak energy density. A representative BS spectrum can be seen in Fig. 2, including the discrete wave components that comprise an irregular wave. Other common wave spectra include the one- and two-parameter Pierson-Moskowitz, ISSC, Liu, JONSWAP, Scott, Ochi-Hubble bimodal, TMA and Mitsuyasu [12]. Potential locations for WEC deployment are not described by a single value for the irregular wave parameters, but rather a set of them. These sets usually are monthly approximations of the parameters [13, 14] or frequency distributions of sea states [14]. Finally, with the wave components characterized, the wave power per unit length is calculated using the following sum:

$$\bar{P} = \sum_{i=1}^{N_I} \frac{1}{16} \rho g^2 \frac{H_i^2}{\omega_i}, \quad (7)$$

where  $\rho = 1025 \text{ kg/m}^3$  is the sea water density and  $g = 9.81 \text{ m/s}^2$  is the gravitational constant.

## 1.2 Design and Control of Wave Energy Converters

Early work in HCWEC design was performed in the frequency domain [2, 7]. This technique requires a number of assumptions, including linearity and regular incident waves. Many authors have stated that there is a fundamental difference between designing WECs for irregular versus regular waves. Drew et al. asserted that a single frequency of the incident sea wave will not predict the performance in real systems [1]. Additionally, Tedeschi et al. emphasized the need to use time-dependent solutions since the instantaneous extracted power in irregular waves is required for realistic analysis [15]. While irregular waves may appear to be a hinderance to WEC design, WECs in irregular waves have the potential to produce better results than WECs in regular waves under similar energy assumptions [16].

Often WEC studies consider both the physical system design (e.g., in this study *a, b*) and the control system design (e.g. feedback controller). This approach is one form of co-design, a class of design methods for integrated physical and control system design that often leads to significant performance improvements [17–20]. A co-design approach is the natural way to handle the WEC design problem since a successful design hinges on exploiting the natural dynamics of the ocean wave–buoy interaction [20, 21].

In this article, WEC design studies will be presented that employ fewer assumptions than many previous investigations. To provide context for understanding these differences, a number of WEC control strategies will be reviewed, followed by a discussion of the various PTO architectures that have been investigated.

**1.2.1 WEC Control Strategies** While passive WECs (i.e. no active control of  $F_{PTO}$ ) can produce energy, incorporating active control increases significantly energy production capability [15, 22, 23], increasing economic competitiveness.

Reactive control was one of the earliest control strategies developed [7]. Under the assumptions of linearity and regular waves, it can be shown that the HCWEC’s dynamic behavior can be described by a second-order transfer function without zeros that will maximize energy production when the optimal velocity is given by:

$$\hat{z}_* = \frac{\hat{F}_e}{2R_r}, \quad (8)$$

where  $\hat{z}_*$  is the complex amplitude of the velocity trajectory,  $\hat{F}_e$  is the excitation force, and  $R_r$  is the radiation resistance (the real part of the WEC radiation impedance, which depends on WEC geometry and wave frequency [7]). Maximum energy production is then produced when velocity is in phase with excitation force, but only when the particularly narrow assumptions described above are valid, including regularity of incident waves. Another important

implication of Eqn. (8) is that a reactive control system—i.e., a PTO is required that can inject energy into the buoy/wave system, not just extract it—is required for optimal energy production. Bidirectional power flow helps exploit natural WEC dynamics [20, 21, 24] to maximize power production. Unfortunately, PTOs capable of bidirectional power flow are difficult to implement in practice. In addition, Tedeschi et al. demonstrated that reactive control in irregular waves is an inferior control strategy [15].

Wave energy extraction can be increased beyond what is possible through optimal control strategies alone. If the physical system is designed such that it resonates with incoming waves, similar to the behavior of electromagnetic antennae or acoustic microphones, energy extraction can be improved [7]. The natural frequency of a heaving point oscillator is given by:

$$\omega_0 = \sqrt{\frac{k_b}{m + m_r(\infty)}} \quad (9)$$

where  $k_b$  is the hydrostatic stiffness,  $m$  is the heaving body mass, and  $m_r(\infty)$  is the infinite-frequency added mass that arises from the motion of radiated waves. Hydrostatic stiffness is a useful model for buoyancy that is analogous to mechanical mass-spring systems; its value depends on buoy geometry.

Since real ocean waves are not regular, WECs cannot simply be designed according to the resonance conditions for a particular frequency. This can be addressed by employing a WEC control system that boosts power production in off-resonance conditions. One intuitive approach proposed by Budal and Falnes involves ‘latching’ the system in place (i.e.  $\dot{z} = 0$  for a short period of time) [2]. The objective of latching control, sometimes referred to as phase control [7, 25, 26], is to keep  $\dot{z}$  and  $F_e$  in phase (or at least to align the extrema of these trajectories with respect to time). This strategy is motivated by the phase requirement for reactive control presented in Eqn. (8). Clement and Babarit showed that a hybrid latching and declutching (freewheeling) control strategy amplified power production substantially, increasing it beyond the sum of the two strategies individually [23].

Optimal control formulations in the time domain have also been studied. These studies often treat buoy velocity as the control input [7, 16, 25]. While PTO force trajectory can be calculated using the results of a velocity-based solution, velocity (or any other system state) cannot be an independent control input. Treating velocity as the control input simplifies solution (e.g., it sidesteps singular optimal control formulations), but the PTO force is a more realistic independent control variable. Clement and Babarit used the simplified PTO model described in Eqn. (10) in formulating an optimal control problem based on Pontrya-

gin's Maximum Principle; the resulting controller exhibited latching behavior [23]. Lattanzio and Scruggs formulated a linear-quadratic-Gaussian (LQG) optimal control problem, finding the optimal casual control for a particular generator arrangement [6]. Direct transcription has also been used to solve WEC problems. Abraham and Kerrigan used a PTO model composed of a linear damper and an active element, resulting in bang-bang control of both control inputs [27]. Allison et al. made no assumptions on PTO architecture to explore the upper limits of HCWEC performance and gain insight into principles of ideal WEC operation in regular ocean waves [8]. Reactive, latching, and declutching behavior all emerged as valid optimal control strategies depending on particular combinations of design and operating constraints.

A variety of suboptimal but more realistic control strategies have been investigated. Valerio et al. have demonstrated a system than switches controllers depending on season [13]. This seems to be a very natural proposition since the sea states widely vary by season. Other methods such as model predictive control [16], internal model control [13], and feedback linearization [13] have been designed for realistic WEC control with varying levels of success. Realistic controller implementations are necessary, but the likelihood of success will depend on the initial controller architecture.

**1.2.2 WEC PTO Architectures** Frequently, the PTO modeling is motivated by reactive control, i.e. modeled as a linear spring-damper system:

$$F_{\text{PTO}} = k_{\text{PTO}}z + R_{\text{PTO}}\dot{z}, \quad (10)$$

where the PTO stiffness  $k_{\text{PTO}}$  corresponds to the capacitive term and the PTO damping  $R_{\text{PTO}}$  corresponds to the dissipative term. Assuming regular wave input, and that these coefficients can be tuned, a PTO design of this form can be found that maximizes energy extraction [23]. The PTO force in Eqn. (10), however, is fundamentally limited in the trajectories in can produce. Many have used this PTO form to provide analytic solutions to a variety of WEC problems [16, 23, 27, 28], but their results are only optimal with respect to the specific simplified PTO architecture. There is no reason to believe that these architectures will produce the true system performance limits.

Realistic PTO systems have been develop that use hydraulics and electric machines. Hydraulic PTOs have been proposed by some due to their ability to absorb energy from the large, slow speeds of ocean waves [1, 26, 29]. Although they are able to drive generators at near constant speeds, they typically suffer from low transmission efficiency. Some have proposed designs based on linear electric machines [3, 5, 28]. This type of PTO has promise since it can provide bidirectional power flow, but in many cases cannot provide compressive (upward) force as it is typically connected via

cables to the buoy. Tedeschi et al. have proposed a PTO where the WEC is attached to a rotational electric machine with power electronics via a gear box [15]. This PTO architecture has many advantages, including the ability to provide bidirectional power flow and PTO force, rendering it an especially promising PTO design strategy.

In this article we make very limited assumptions on the PTO architecture; thus, the linear PTO restriction has been removed, similar to the work performed in Ref. [8]. In the following section we will outline our co-design problem formulation including the system model. Finally, some results and parametric studies will be presented.

## 2 Co-Design Problem Formulation

A co-design problem formulation is defined here to provide a means for solving the energy maximization problem. The general co-design problem with a Bolza objective is:

$$\begin{aligned} \min_{\boldsymbol{\xi}, \mathbf{u}, \mathbf{x}_p} \quad & \Psi = \Phi(\boldsymbol{\xi}(t_0), t_0, \boldsymbol{\xi}(t_f), t_f, \mathbf{x}_p) \\ & + \int_{t_0}^{t_f} \mathcal{L}(\boldsymbol{\xi}(t), \mathbf{u}(t), t, \mathbf{x}_p) dt \end{aligned} \quad (11a)$$

subject to :

$$\dot{\boldsymbol{\xi}}(t) = \mathbf{f}_d(\boldsymbol{\xi}(t), \mathbf{u}(t), t, \mathbf{x}_p) \quad (11b)$$

$$\boldsymbol{\phi}_{\min} \leq \boldsymbol{\phi}(\boldsymbol{\xi}(t_0), t_0, \boldsymbol{\xi}(t_f), t_f, \mathbf{x}_p) \leq \boldsymbol{\phi}_{\max} \quad (11c)$$

$$\mathbf{C}_{\min} \leq \mathbf{C}(\boldsymbol{\xi}(t), \mathbf{u}(t), t, \mathbf{x}_p) \leq \mathbf{C}_{\max} \quad (11d)$$

where  $\boldsymbol{\xi}(t)$ ,  $\mathbf{u}(t)$ ,  $\mathbf{x}_p = [a, b]^T$ , and  $t$  represent, respectively, the state, control, plant design variables, and time [30–32]. Eqn. (11a) is the cost functional that is to be minimized. The dynamic constraints are given in Eqn. (11b). The boundary constraints are given in Eqn. (11c), and the inequality path constraints are given in Eqn. (11d). These two equations also include all necessary plant design constraints (Eqn. (11c) is used for time-independent plant constraints and Eqn. (11d) is used for constraints that need collocation).

### 2.1 Dynamic Constraints

The dynamic system model used in this article is similar to the one described in Ref. [33]. The equation of motion for the HCWEC in Fig. 1 can be written as

$$m\ddot{z} + F_e + F_r + F_v + F_b + F_{\text{PTO}} = 0, \quad (12)$$

where  $F_e$  is the excitation force,  $F_r$  is the radiation force,  $F_v$  is the viscous force, and  $F_b$  is the buoyancy force. The excitation force in irregular waves for bodies with a vertical

axis of symmetry oscillating in heave is given by

$$F_e = \sum_{i=1}^{N_I} \sqrt{\frac{\rho g^3 R_r(\omega_i)}{2\omega_i^3}} \eta_i(t). \quad (13)$$

The radiation force can be modeled as:

$$F_r = m_r(\infty)\dot{z} + \int_0^t L(t-\tau)\dot{z}(\tau)d\tau, \quad (14)$$

where  $L(t)$  is the fluid-memory model. This term incorporates the energy dissipation due to waves generated by the body motion [33]. The fluid-memory model is

$$L(t) = \frac{2}{\pi} \int_0^\infty \frac{R_r(\omega)}{\omega} \sin(\omega t) d\omega. \quad (15)$$

The radiation force (along with  $F_e$  and  $R_r$ ) can be computed using wave interaction software [34]. Models that incorporate the convolution integral in Eqn. (14) are challenging to use with existing optimization algorithms as this integral results in integro-differential equations that are computationally expensive to simulate. In this study, the radiation damping term will be approximated with a linear term,  $\bar{R}_r$ , using weights based on  $S(\omega)$ :

$$\bar{R}_r = \sum_{i=1}^{N_I} \frac{R_r(\omega_i)S(\omega_i)\Delta\omega_i}{\sum_{i=1}^{N_I} S(\omega_i)\Delta\omega_i} \quad (16)$$

Future studies will address the integral term through the development of methods that support efficient direct calculation.

The buoyancy force is proportional to the submersion depth, and due to its constant cross-sectional area is given by the following formula:

$$F_b = g\rho\pi a^2 z = k_b z. \quad (17)$$

Finally, the viscous force will be approximated using the linearized drag force:

$$F_v = 0.5C_D\rho\pi a^2 \dot{z}_{\max}\dot{z} = R_v \dot{z}, \quad (18)$$

where  $C_D = 0.81$  is the drag coefficient [35], and  $\dot{z}_{\max} = 3$  m/s is the approximate maximum velocity of the HCWEC. With all the forces defined, the general state space model can be written as

$$\dot{\boldsymbol{\xi}} = \mathbf{A}\boldsymbol{\xi} + \mathbf{B}\mathbf{u} + \mathbf{K}\mathbf{e}, \quad (19)$$

where:

$$\mathbf{A} = \begin{bmatrix} 0 & a_{12} \\ a_{21} & a_{22} \end{bmatrix}, \quad \mathbf{B} = \begin{bmatrix} 0 \\ b_{21} \end{bmatrix}, \quad \mathbf{K} = \begin{bmatrix} 0 \\ k_{21} \end{bmatrix},$$

$$\boldsymbol{\xi} = \begin{bmatrix} z(t) \\ \dot{z}(t) \end{bmatrix}, \quad u = F_{\text{PTO}}(t), \quad e = F_e(t),$$

$$a_{21} = \frac{-k_b}{m + m_r(\infty)}, \quad a_{22} = \frac{-(\bar{R}_r + R_v)}{m + m_r(\infty)}, \quad a_{12} = 1,$$

$$b_{21} = \frac{-1}{m + m_r(\infty)}, \quad k_{21} = \frac{-1}{m + m_r(\infty)}.$$

## 2.2 Objective Function

The maximization of energy production over a finite time interval  $0 \rightarrow T$  requires only the running cost term of the Bolza objective,  $\mathcal{L}(\cdot)$ . However, an additional quadratic penalty term has been added since the control input appears linearly in the Hamiltonian:

$$H(\mathbf{p}, \boldsymbol{\xi}, u, t) = \xi_2 u + \mathbf{p}^T (\mathbf{A}\boldsymbol{\xi} + \mathbf{B}\mathbf{u} + \mathbf{K}\mathbf{e}), \quad (20)$$

where  $\mathbf{p}$  is the costate vector. Consequently, maximizing energy production with respect to  $F_{\text{PTO}}(t)$  is a singular optimal control problem (which is difficult, but possible to solve) [32]. Kasturi and Dupont added a quadratic penalty term to an analogous mass-spring-damper system to enable efficient solution [36]. Clement and Babarit also noted that their WEC system design problem was a singular optimal control problem [23]. The optimization formulation (unconstrained version) used here is:

$$\min_{\boldsymbol{\xi}, \mathbf{u}, \mathbf{x}_p} - \int_0^T (\dot{z}(t)F_{\text{PTO}}(t) + R_{\text{pen}}[F_{\text{PTO}}(t)]^2) dt, \quad (21)$$

where  $R_{\text{pen}} \in \mathbb{R}_{\geq 0}$  is the penalty weight. The addition of the penalty term perturbs the underlining problem, so using the smallest possible value of  $R_{\text{pen}}$  that still facilitates solution is desirable. It is analogous to the energy required for the PTO to make control decisions. The general strategy used to find  $R_{\text{pen}}$  follows: select a large initial value, solve Prob. (21), then iteratively decrease it by a power of 10 until the results appear to be physically improbable (i.e., unintuitively fast dynamics). A general rule is to attempt to adjust the penalty term to a value significantly smaller than the original objective term ( $|\dot{z}F_{\text{PTO}}| > |R_{\text{pen}}F_{\text{PTO}}^2, \forall t$ ).

## 2.3 Boundary Constraints

**2.3.1 Periodic Constraints** Irregular waves are periodic since they are a sum of periodic components. Typically, a few frequencies in wave spectrum are dominant as evident in  $S(\omega)$ . Using these dominant frequencies, an approximation for the period of the irregular wave can be found. For the solution to be periodic as well, the states must be the same at the initial and final time (written in a form consistent with Eqn. (11c)):

$$\mathbf{0} \leq \boldsymbol{\xi}(T) - \boldsymbol{\xi}(0) \leq \mathbf{0}. \quad (22)$$

Adding this constraint results in a periodic optimal control problem, which arises in various applications including vibrating systems [36] and aircraft cruise control [37]. Using a periodic optimal control approach for the design of WEC control systems in irregular waves greatly reduces the computational expense when compared to the conventional strategy of using a large time horizon.

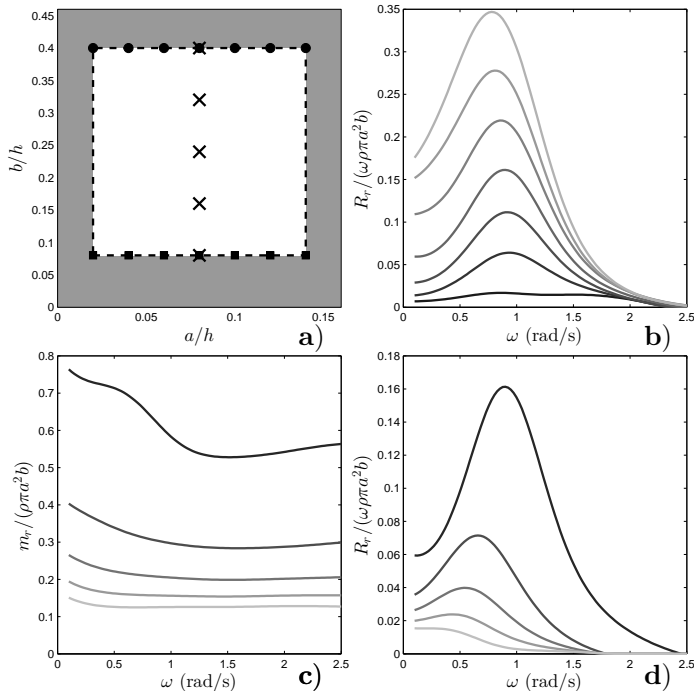


**FIGURE 3:** a) Design space of  $a/h$  and  $b/h$  with data points  $\blacksquare$ ,  $\bullet$  from [14], white feasible region, all curves drawn using neural network, darker lines indicate smaller geometric ratio b)  $R_r(\omega)$  using  $\blacksquare$  points c)  $m_r(\omega)$  using  $\times$  points d)  $R_r(\omega)$  using  $\times$  points.

**2.3.2 Time-Independent Plant Constraints** The mass of the HCWEC is equivalent to the submerged mass:

$$m = \rho \pi a^2 b. \quad (23)$$

The geometric design variables can be nondimensionalized as  $a/h$  and  $b/h$ . Closed-form solutions of  $R_r(\omega)$  and  $m_r(\omega)$  for a floating circular cylinder in finite-depth water have been found [38]. Data was taken from Ref. [14] and modeled using an artificial neural network (ANN) with 10 hidden layers. The objective used when fitting the ANN was to preserve the shape of the curves with the modeled points. Since a finite number of data points were used (14 curves for each coefficient), input constraints are needed to preserve model accuracy.

$$0.02 \leq a/h \leq 0.14 \quad 0.08 \leq b/h \leq 0.40 \quad (24)$$

The derivation is based on the data points locations shown in Fig. 3a. Fig. 3b demonstrates the effect of  $a$  on  $R_r(\omega)$ . Fig. 3c and Fig. 3d show the effect of  $b$  on both  $m_r(\omega)$  and  $R_r(\omega)$ . Note that the 3 inner curves are at completely different locations than the collected data points.

**TABLE 1:** Four Design Cases.

Case	$C_{\min}$	$u_{\min}$	
1	$-\infty$	$-\infty$	Unconstrained
2	$-\infty$	0	No compr. PTO force
3	0	$-\infty$	No reactive power
4	0	0	Both constraints

## 2.4 Inequality Path Constraints

**2.4.1 Position Constraint** If the buoy completely leaves the water it will impact the water on its way back down. This slamming of the HCWEC should be avoided. The following constraint prevents this event:

$$z(t) - (\eta(t) + b) \leq 0. \quad (25)$$

**2.4.2 Power Constraint** Practical PTOs (at least so far) cannot provide bidirectional power flow [7]. Therefore, we would like to study the effects on applying a power inequality path constraint on the PTO force trajectory:

$$C_{\min} \leq \dot{z}(t) F_{\text{PTO}}(t) \leq \infty, \quad (26)$$

where  $C_{\min}$  can be either  $-\infty$  or 0.

**2.4.3 Control Force Constraint** Asymmetric control input bounds should be considered. In most previous studies no explicit control input bounds (e.g.,  $u_{\min} \leq u \leq u_{\max}$ ) are employed, although Hals and Faldes imposed symmetric PTO force constraints [16]. Asymmetric constraints (e.g.,  $0 \leq F_{\text{PTO}} \leq F_{\max}$ ) are useful for modeling WECs where an upward force cannot be exerted on the buoy because of a cable connection between the buoy and the PTO. Asymmetric constraints are difficult to implement using conventional optimal control methods, highlighting the value of the direct optimal control methods such as direct transcription or pseudospectral methods (introduced in the next subsection). In this article, four different combinations of the power and control input constraints are considered (see Table 1).

## 2.5 Solving Optimal Control Problems with Pseudospectral Methods

Several options exist for solving the HCWEC optimal control problem described above. Here the solution was implemented using the General Pseudospectral Optimization Software (GPOPS) Version 5.1 [31], which uses the Radau Pseudospectral Method (RPM) with Legendre-Gauss-Radau (LGR) collocation points and an  $hp$ -adaptive mesh refinement algorithm. GPOPS has been used to solve a wide variety of optimal control problems including chemotherapy treatment [39] and spacecraft trajectory

design [40]. The RPM is a direct method where the optimality conditions are not explicitly derived. Instead, state and control trajectories are parametrized using function approximation, and the cost is approximated using a quadrature method. This converts the infinite-dimensional problem into a finite one, i.e. a nonlinear program (NLP). This is an open-loop control design method, i.e. we have complete freedom when designing the control trajectory. Direct methods create a large number of algebraic equations that ensure physics are satisfied at each time step. These equations are known as defect constraints. The particular form of these constraints used in pseudospectral methods is

$$\sum_{i=0}^N \mathbf{D}_{ki} \Xi - \mathbf{f}_d(\Xi, \mathbf{U}, t, \mathbf{x}_p) = \mathbf{0} \quad (k = 1, \dots, N), \quad (27)$$

where  $D_{ki}$  is the differentiation matrix representing the Lagrange interpolating polynomial,  $\Xi$  is the matrix of discretized states,  $\mathbf{U}$  is the matrix of discretized control trajectories, and  $N$  is the degree of the polynomial. When Eqn. (27) is satisfied, the interpolating polynomial correctly models the dynamic system.

### 3 Numerical Results

Numerical experiments were performed for all four cases using GPOPS. Additional parametric studies on the bounds of the instantaneous power and velocity were also performed.

#### 3.1 Case Results

The results are performed on a hypothetical location with  $h = 10$  m described by the Bretschneider spectrum with  $H_{1/3} = 4$  m and  $T_p = 8$  s. The phases were randomly calculated for the 21 wave components used to construct  $\eta$  over the range of 0.5 rad/s to 2.5 rad/s with  $\Delta\omega = 0.1$  rad/s. Our time horizon was determined to be  $T = 63$  s by visually approximating the periodicity of the wave (see Fig. 2b or  $\eta$  in the cases). Since no constraints were directly placed on the velocity, it was limited to  $\pm 3$  m/s as high velocities are hazardous to WEC operation [1].

The  $R_{\text{pen}}$  was set at  $5 \times 10^{-5}$ . When the parameter was reduced too far, bang–bang solutions resulted, which is expected in a singular optimal control problem. These bang–bang solutions, however, had impractically fast switching behavior. In contrast, excessively large values for the penalty parameter degraded energy production since a large penalty resulted in low PTO force.

Initial studies employed a simultaneous co-design approach, optimizing the plant design variables and control simultaneously [30]. Solution difficulty was too high with this approach so nested co-design was employed. Paramet-

TABLE 2: Case Results.

	Case 1	Case 2	Case 3	Case 4
$a$	0.59 m	0.39 m	1.40 m	1.40 m
$b$	1.71 m	0.80 m	0.80 m	1.09 m
$m$	1917 kg	392 kg	5049 kg	6880 kg
$m_r(\infty)$	413 kg	117 kg	4749 kg	5118 kg
$T$	2.89 s	2.04 s	2.50 s	2.77 s
$P_{\text{avg}}$	1.89 kW	1.30 kW	2.56 kW	1.97 kW

ric sweeps of  $(a, b)$  were performed for all four test cases. In these sweeps, control was optimized for every pair considered. In Fig. 4 the percentage of available energy extracted is shown. Adding more constraints (Case 4 has the most constraints) increased numerical difficulties, as evidenced by the numerical noise in Cases 3 and 4. The location of maximum energy extraction for each case is denoted by a white dot. Table 2 characterizes each of these solutions. The wave elevation (top-dashed), position (top-solid), velocity (middle-dashed), PTO force (middle-solid), and instantaneous power (bottom-solid) are plotted for each of the four cases in Figs. 5–8. For this particular irregular wave, the wave power per unit length was 13.4 kW/m, calculated using Eqn. (7), while  $P_{\text{avg}}$  ranged from 10% to 19% of this value.

The expected relative results of the average power extracted were  $P_1 > P_3 > P_2 > P_4$  [8]. Case 1 is unconstrained (or the most unconstrained); therefore should have the largest  $P$ . Similarly,  $P_4$  must be the smallest since it is the most constrained. Analyzing these results,  $P_1 > P_2$  and  $P_3 > P_4$ , implying the PTO force constraint is indeed deteriorating the energy extraction. Adding the power constraint does not produce the expected result. We have already discussed guidelines for setting  $R_{\text{pen}}$ . However, due to solution difficulty, the value used was quite high in order to produce physically meaningful solutions. This caused the quadratic cost term to dominate power term in Eqn. (21). Therefore, solutions found in Cases 2-4 were actually worse than using no control at all (i.e., the value of Eqn. (21) was positive while a solution with zero control would result in a zero value). On the other hand, Case 1 produced a modified objective function value that was indeed negative. This raises two questions regarding the algorithm’s desire to choose solutions with positive modified objective values and solution relevance. Addressing the first point, the initial mesh (collection of the discrete time points) was undefined so GPOPS’s mesh refinement algorithm iteratively creates it. In addition, the initial values for the states and control were zero-valued. Therefore, it seems like the zero-valued

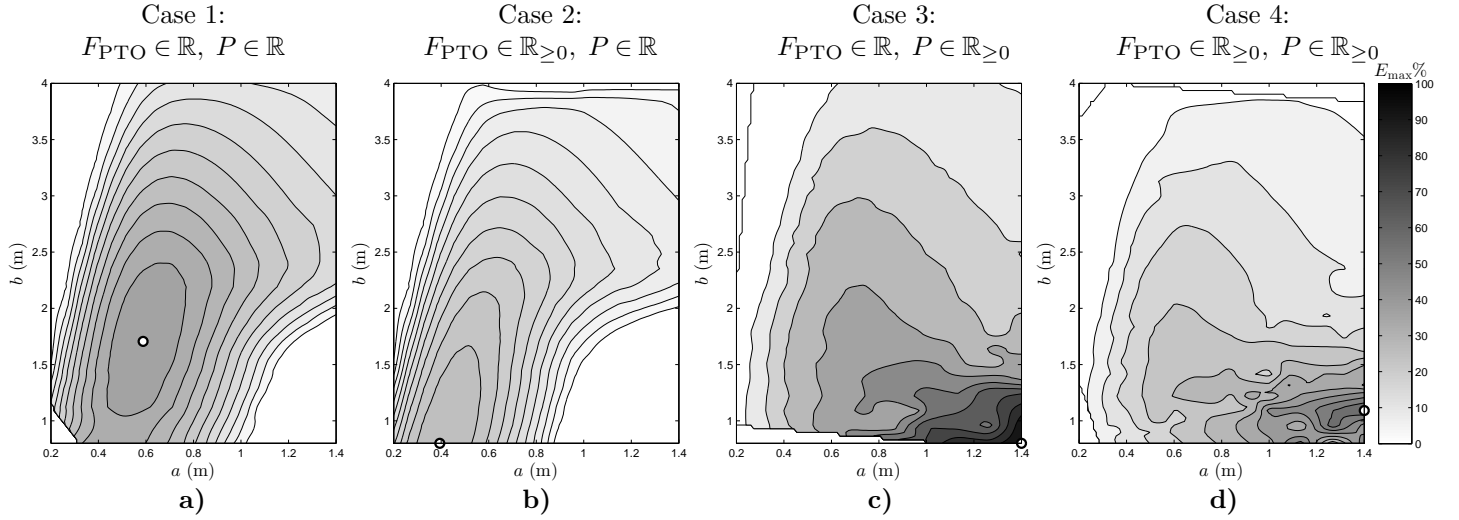


FIGURE 4: Design Space of the HCWEC for All Four Cases.

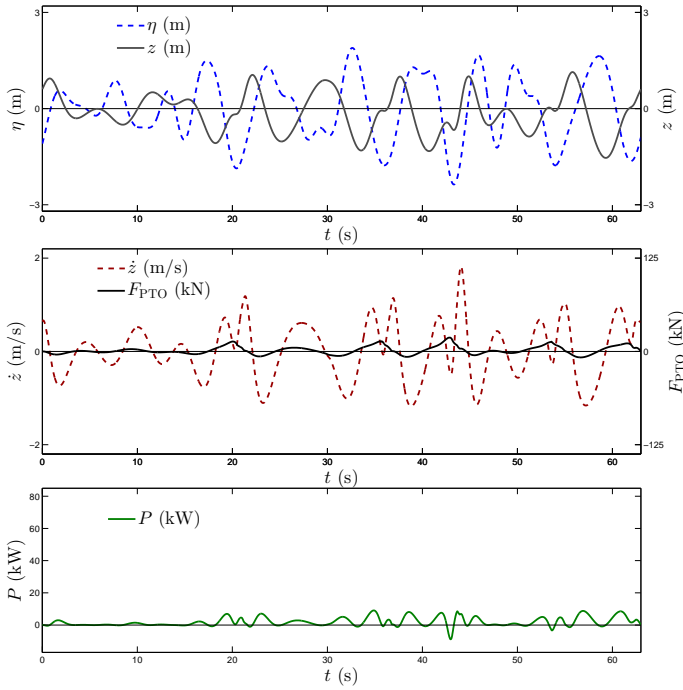


FIGURE 5: Case 1 Results.

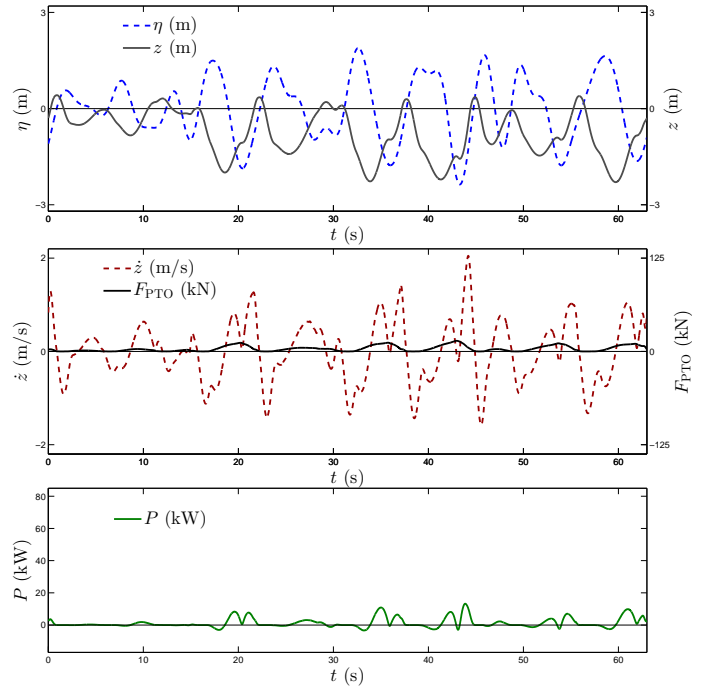


FIGURE 6: Case 2 Results.

solution should have been found. We suspect that Cases 2-4 are local solutions. All of this implies that the penalty parameter was too high and since it could not be reduced, the method used to avoid the singular optimal control aspect was poor. This motivates the development of new methods to account for this issue.

Even with all discussed issues with the solutions, these feasible solutions provide design insights since they were seeking the optimal energy extraction. For this point on, it is important to remember that no design guidelines were provided, only an objective and constraints. Therefore, all phenomena that arise are due to the desired natural dynam-



ics of the system.

WEC behavior, based on the optimal design for each case, will now be explored. Case 1 exhibits locally harmonic solutions for both the state and control (Fig. 5). A small amount of reactive power ( $P < 0$ ) is observed, particularly around the more dynamic sections of the incoming wave. The constraint in Eqn. (25) becomes active a number of times. There are no large periods of constant position that would indicate latching behavior, or periods of zero control force (declutching). Finally, the necessary condition that all the trajectories are periodic is satisfied. In Case 2, shown in Fig. 6, a large number of zero-valued control regions are observed. Declutching, therefore, is a necessary control strategy when the PTO force constraint is active. Similar to Case 1, many locally harmonic solutions were found when declutching was not active.

For Cases 3 and 4, no reactive power was observed due to the active power constraint (except in a few minor locations where negative power exists within the algorithm tolerance). The solutions in these cases were largely non-harmonic. Declutching is apparent in Cases 3 and 4, although more abundant in Case 4 with the addition of the PTO force constraint. Interestingly, latching was quite prevalent. For at least a third of the wave, the device was latching. The device was released at the lowest points of the wave, supporting previous work based on the objective of keeping the excitation force and a device in phase [2, 7, 25, 26]. To summarize, the PTO force constraint had the following effect: declutching, limited time extracting power, and larger peak instantaneous power.

Finally, since the irregular wave was characterized by a single period, one might postulate that this is the optimal natural period of the HCWEC. This statement is true in regular waves [7]. Using Eqns. (9), (17), and (23) while nondimensionalizing the added mass coefficient to  $\mu(\omega_0) = m_r(\omega_0)/(\rho\pi a^2 b)$ , the optimal draft can be calculated such that the HCWEC resonates with the incoming regular wave:

$$b = \frac{g}{\omega_0^2 (1 + \mu(\infty))}. \quad (28)$$

This is consistent with statements in Ref. [7]. The maximum value  $\mu(\infty)$  attains in our feasible design space is  $\approx 0.94$ . The modal angular frequency for our study was  $2\pi/T_p = 0.79$  rad/s. Therefore, the smallest possible  $b$  would be 8.2 m, which is outside our current feasible design space. However, the results are not trending toward large values of  $b$  but smaller ones. Smaller  $b$  values indicate higher frequency (or lower period) devices. The optimal periods for each case can be seen in Table 2 with a range of 2.04 s to 2.77s. Therefore, much higher frequencies (or lower periods) are preferred relative to the modal period. Higher frequency WECs can respond more rapidly to ac-

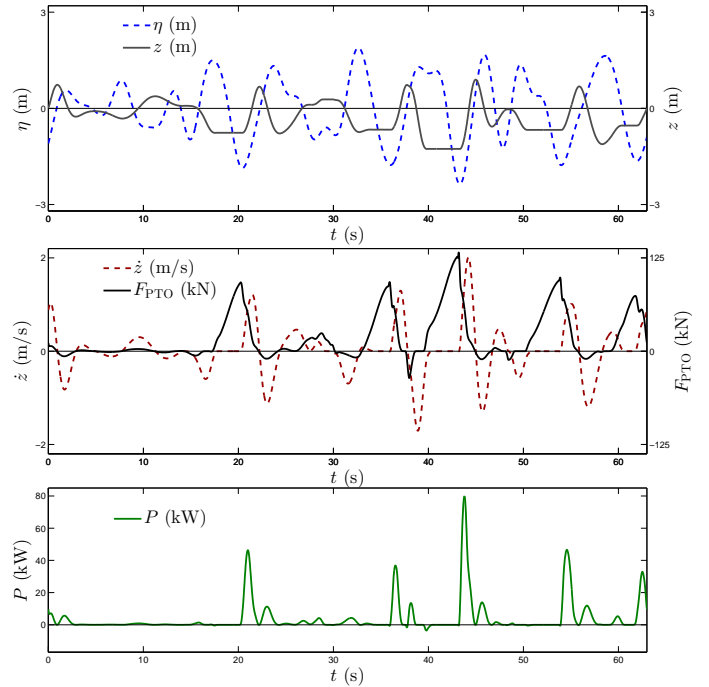


FIGURE 7: Case 3 Results.

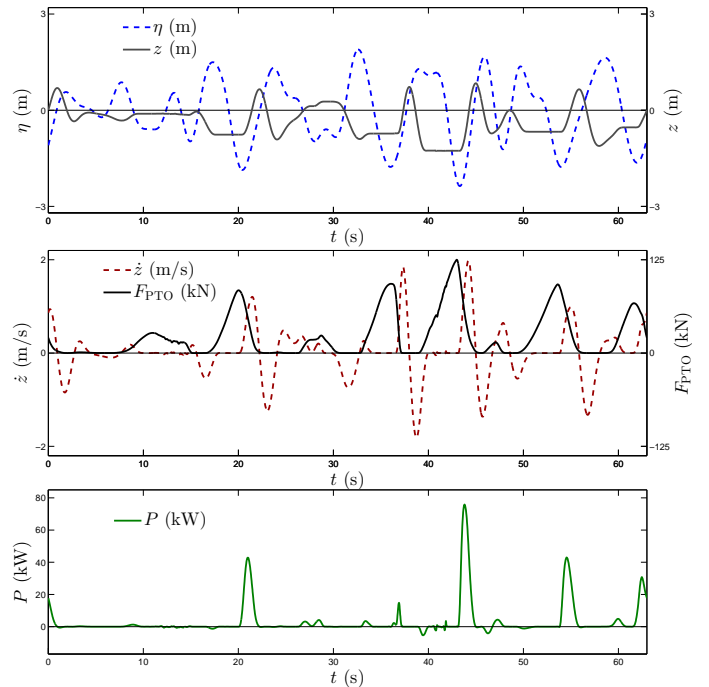


FIGURE 8: Case 4 Results.

tive control. In addition, HCWEC performance in irregular waves is quite poor in off-resonance conditions, but  $> 40\%$  of the maximum energy production is possible with variety of low-period buoy designs.

### 3.2 Parametric Studies

A WEC PTO must handle the largest value of the instantaneous power that may occur, adding to system expense, and potentially sacrificing its cost to production ratio. A power constraint (i.e.  $C_{\max} \leq \gamma$ ,  $\gamma$  is the maximum allowed power) was added to Case 1 to investigate this practical design issue. This bound was varied from 10 kW down to 0 kW. The results are shown in Fig. 9a. As expected, energy extraction decreases with  $\gamma$ . Increasing  $\gamma$  beyond 8 kW does not improve energy performance noticeably. In fact, when the maximum power is limited to  $C_{\max} = 3.3$  kW, the energy production is still 80% of the maximum, potentially improving the energy/cost ratio. To illustrate system behavior more clearly, the power trajectory is plotted for a few select values of  $\gamma$  in Fig. 9b. As the maximum power  $C_{\max}$  is reduced, flat spots appear at the power bound. The width of these flat spots increases with decreasing  $C_{\max}$ , allowing the WEC to produce more energy than if the power trajectory for the unconstrained case was simply “cut” at the bound. In addition to reducing PTO power requirements, introducing the power bound results in a more consistent power level, which is desirable for grid integration.

A parametric study was also performed on the velocity bound. The tradeoff between maximum velocity and energy extraction exhibited trend similar to the  $C_{\max}$  vs.  $P$  relationship shown in Fig. 9a.

### 4 Conclusion

A significant amount of work has been performed in the field of wave energy conversion. Both regular and irregular waves are often considered, but predicting performance in real ocean waves requires consideration of irregular waves. Many detailed studies have addressed PTO design, although assumptions commonly made in these studies restrict potential PTO designs. In this article a co-design formulation was proposed with few PTO restrictions. Co-design using direct transcription was an enabling technology for the studies presented here. Even with the presence of numerical difficulties, this approach provided insight into the natural trajectories that maximize energy extraction. Parametric studies were performed to explore the trade-offs between energy production and cost. WEC designs with unconstrained PTO control present many implementation challenges, motivating the detailed study of the effects of PTO force, power, and velocity bounds.

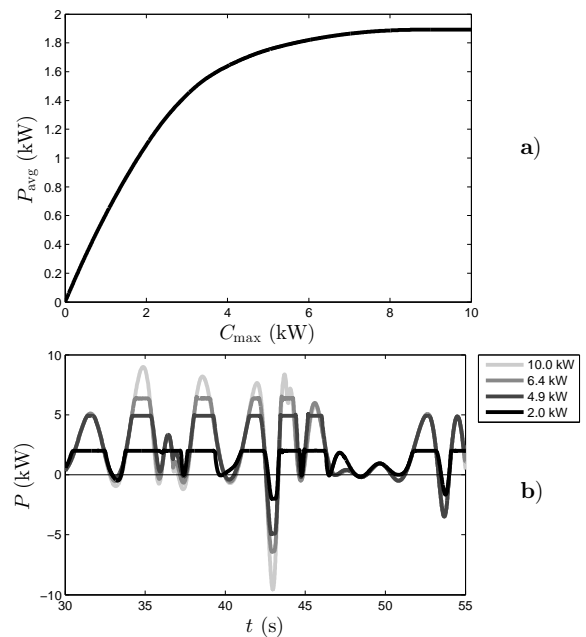


**FIGURE 9:** a) Energy extraction vs.  $C_{\max}$  for Case 1 b) Power trajectory for various levels of  $C_{\max}$ .

Results of this investigation led to several important conclusions: a) the frequency calculated with the optimal plant design is higher than the modal period, b) a higher percentage of available energy can be extracted in off-resonance conditions in irregular waves than comparable regular waves, c) the path constraint preventing the slamming of the device is active, d) both declutching and latching control strategies were present in the suboptimal cases (Cases 2–4), and e) realistic trade-offs with energy production can be made with respect to the maximum instantaneous power or velocity to improve cost-effectiveness.

### REFERENCES

- [1] Drew, B., Plummer, A., and Sahinkaya, M., 2009. “A Review of Wave Energy Converter Technology”. In the Proceedings of the Institution of Mechanical Engineers, Part A: Journal of Power and Energy, Vol. 223, pp. 887–902.
- [2] Budal, K., and Falnes, J., 1980. “Interacting Point Absorbers with Controlled Motion”. In *Power from Sea Waves*, B. Count, ed. Academic Press, pp. 381–399.
- [3] Eriksson, M., 2007. “Modelling and Experimental Verification of Direct Drive Wave Energy Conversion”. Ph.D. dissertation, Uppsala University.
- [4] Falnes, J., 2007. “A Review of Wave-Energy Extraction”. *Marine Structures*, **20**(4), Oct., pp. 185–201.
- [5] Ivanova, I. A., Bernhoff, H., Ågren, O., and Leijon, M., 2005. “Simulated Generator for Wave Energy Extraction in Deep Water”. *Ocean Engineering*, **32**(14-15), Oct., pp. 1664–1678.
- [6] Lattanzio, S. M., and Scruggs, J. T., 2011. “Maximum Power

- Generation of a Wave Energy Converter in a Stochastic Environment”. In the Proceedings of the 2011 IEEE International Conference on Control Applications, IEEE, pp. 1125–1130.
- [7] Falnes, J., 2002. *Wave-Energy Absorption by Oscillating Bodies*. Cambridge University Press.
- [8] Allison, J. T., Kaitharath, A., and Herber, D. R., 2012. “Wave Energy Extraction Maximization Using Direct Transcription”. In the Proceedings of the ASME 2012 International Mechanical Engineering Congress & Exposition, no. IMECE2012-86619, ASME.
- [9] Jeans, T., Fagley, C., Siegel, S., and Seidel, J., 2011. “Irregular Deep Ocean Wave Energy Conversion Using a Cycloidal Wave Energy Converter”. In the Proceedings of the 9th European Wave and Tidal Energy Conference.
- [10] McTaggart, K., 2003. Modelling and Simulation of Seaways in Deep Water for Simulation of Ship Motions. Tech. Rep. DRDC-ATLANTIC-TM-2003-190, Defence R&D Canada, Sept.
- [11] McCormick, M., 1981. *Oceans Wave Energy Conversion*. Wiley.
- [12] ITTC, 2002. “The Specialist Committee on Waves — Final Report and Recommendations to the 23rd ITTC”. In the Proceedings of the 23rd International Towing Tank Conference, Vol. 2, pp. 505–551.
- [13] Valerio, D., Beirao, P., Mendes, M. J. G., and Sa da Costa, J., 2008. “Comparison of Control Strategies Performance for a Wave Energy Converter”. In the Proceedings of the 2008 Mediterranean Conference on Control and Automation, pp. 773–778.
- [14] Bachynski, E. E., Young, Y. L., and Yeung, R. W., 2012. “Analysis and Optimization of a Tethered Wave Energy Converter in Irregular Waves”. *Renewable Energy*, **48**, pp. 133–145.
- [15] Tedeschi, E., Molinas, M., Carraro, M., and Mattavelli, P., 2010. “Analysis of Power Extraction from Irregular Waves by All-Electric Power Take Off”. In the Proceedings of the 2010 IEEE Energy Conversion Congress and Exposition, IEEE, pp. 2370–2377.
- [16] Hals, J., Falnes, J., and Moan, T., 2011. “Constrained Optimal Control of a Heaving Buoy Wave-Energy Converter”. *Journal of Offshore Mechanics and Arctic Engineering*, **133**(1), p. 011401.
- [17] Fathy, H., 2003. “Combined Plant and Control Optimization: Theory, Strategies and Applications”. Ph.D. dissertation, University of Michigan.
- [18] Allison, J., and Nazari, S., 2010. “Combined Plant and Controller Design Using Decomposition-Based Design Optimization and the Minimum Principle”. In the Proceedings of the 2010 ASME Design Engineering Technical Conference, no. DETC2010-28887, ASME.
- [19] Allison, J., and Han, Z., 2011. “Co-Design of an Active Suspension Using Simultaneous Dynamic Optimization”. In the Proceedings of the 2011 ASME Design Engineering Technical Conference, no. DETC2011-48521, ASME.
- [20] Allison, J., 2012. “Plant-Limited Co-Design of an Energy Efficient Counterbalanced Robotic Manipulator”. In the Proceedings of the 2012 ASME Design Engineering Technical Conference, no. DETC2012-71108, ASME.
- [21] Allison, J., 2012. “Engineering System Co-Design with Limited Plant Redesign”. In the Proceedings of the 8th AIAA Multidisciplinary Design Optimization Specialist Conference, AIAA.
- [22] Korde, U., 2000. “Control System Applications in Wave Energy Conversion”. In the Proceedings of the OCEANS 2000 MTS/IEEE Conference and Exhibition, Vol. 3, pp. 1817–1824.
- [23] Clément, A. H., and Babarit, A., 2012. “Discrete Control of Resonant Wave Energy Devices”. *Philosophical Transactions of the Royal Society A: Mathematical, Physical and Engineering Sciences*, **370**(1959), Jan., pp. 288–314.
- [24] Pitti, A., and Lungarella, M., 2006. “Exploration of Natural Dynamics Through Resonance and Chaos”. In the Proceedings of the 9th Conference on Intelligent Autonomous Systems, pp. 558–565.
- [25] Falnes, J., and Hals, J., 2012. “Heaving Buoys, Point Absorbers and Arrays”. *Philosophical Transactions of the Royal Society A: Mathematical, Physical and Engineering Sciences*, **370**(1959), Jan., pp. 246–77.
- [26] Falcão, A. F. D. O., 2008. “Phase Control Through Load Control of Oscillating-Body Wave Energy Converters with Hydraulic PTO System”. *Ocean Engineering*, **35**(3-4), Mar., pp. 358–366.
- [27] Abraham, E., and Kerrigan, E. C., 2013. “Optimal Active Control and Optimization of a Wave Energy Converter”. *IEEE Transactions on Sustainable Energy*, **4**(2), pp. 324–332.
- [28] Santana, A. G., El, D., Andrade, M., De, A., Jaén, V., and Ingeniería, A. G., 2010. “Control of Hydrodynamic Parameters of Wave Energy Point Absorbers using Linear Generators and VSC-based Power Converters Connected to the Grid”. In the International Conference on Renewable Energies and Power Quality.
- [29] Ringwood, J., 2008. “Practical Challenges in Harvesting Wave Energy”. In the Proceedings ECOR Symposium.
- [30] Allison, J. T., and Herber, D. R., 2013. “Multidisciplinary Design Optimization of Dynamic Engineering Systems”. *AIAA Journal*, to appear.
- [31] Rao, A. V., Benson, D. A., Darby, C. L., Patterson, M. A., Francolin, C., Sanders, I., and Huntington, G. T., 2012. “Algorithm 902: GPOPS, A MATLAB Software for Solving Multiple-Phase Optimal Control Problems Using The Gauss Pseudospectral Method”. *ACM Transactions on Mathematical Software*, **37**(2), Apr./June, pp. 1–39. Article No. 22.
- [32] Betts, J. T., 2010. *Practical Methods for Optimal Control and Estimation Using Nonlinear Programming*. SIAM.
- [33] Journée, J. M. J., and Massie, W. W., 2001. *Offshore Hydrodynamics*, first ed. Delft University of Technology, Jan. Chapter 6 Rigid Body Dynamics.
- [34] Lee, C. H., and Newman, J. N. *WAMIT<sup>®</sup> User Manual, Version 7.0*. <http://www.wamit.com/>.
- [35] Hoerner, S., 1965. *Fluid Dynamic Drag*. Hoerner Fluid Dynamics.
- [36] Kasturi, P., and Dupont, P., 1998. “Constrained Optimal Control of Vibration Dampers”. *Journal of Sound and Vibration*, **215**(3), pp. 499–509.
- [37] Speyer, J. L., 1996. “Periodic Optimal Flight”. *Journal of Guidance, Control, and Dynamics*, **19**(4), pp. 745–755.
- [38] Yeung, R. W., 1981. “Added Mass and Damping of a Vertical Cylinder in Finite-Depth Waters”. *Applied Ocean Research*, **4**(3), pp. 119–133.
- [39] Ledzewicz, U., Naghnaeian, M., and Schaettler, H., 2012. “Optimal Response to Chemotherapy for a Mathematical Model in Tumor-Immune Dynamics”. *Journal of Mathematical Biology*, **64**(3), Feb., pp. 557–577.
- [40] Darby, C. L., and Rao, A. V., 2011. “Minimum-Fuel Low-Earth Orbit Aeroassisted Orbital Transfer of Small Spacecraft”. *Journal of Spacecraft and Rockets*, **48**(4), July/Aug., pp. 618–628.